Symmetry and strain-induced effects at the W point of the Brillouin zone of face-centered-cubic crystals

G. C. La Rocca, U. Schmid, and M. Cardona
Max-Planck-Institut für Festkörperforschung, Heisenbergstrasse 1, D-7000 Stuttgart 80, Federal Republic of Germany
(Received 5 February 1991)

The invariant expansions of the effective-mass Hamiltonian at the W point of fcc crystals including strain interactions are presented for the space groups $Fm3m$ (O_h^5), $Fd3m$ (O_h^7), and $F\bar{4}3m$ (T_d^2). The intervalley and intravalley splittings induced by uniaxial stress along high-symmetry directions are derived for both phonon and electron spectra. Relevant parameters for the electronic bands of germanium near W are calculated with the *ab initio* linear-muffin-tin-orbital method.

I. INTRODUCTION

The spectra of elementary excitations in solids exhibit strong features corresponding to the critical points of their dispersion relations.[1] The crystal symmetry determines (almost completely) the location of critical points and the shape of the bands in their vicinity, as well as how they are modified in the presence of an external perturbation.[2] The effective-mass theory, combined with group-theoretical symmetry considerations, provides much guidance in the investigation of these properties, especially when the application of a magnetic field or uniaxial stress brings about qualitative changes in the spectra.[3–6] In face-centered-cubic crystals, critical points are required to occur at the Γ, L, X, and W points of the Brillouin zone (see Fig. 1).[7] Among those, the W point is the less extensively investigated. W-related features are often experimentally elusive and sometimes controversial.[8]

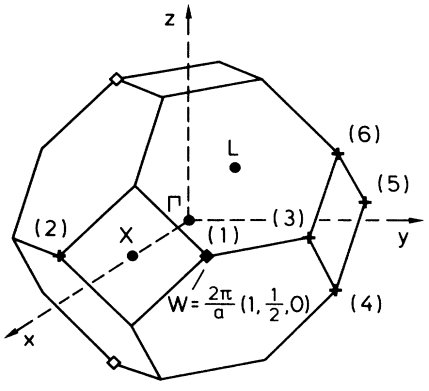

FIG. 1. Brillouin zone of face-centered-cubic lattice. The full diamond indicates the representative W point at $(2\pi/a)(1,\frac{1}{2},0)$ (the two empty diamonds correspond to equivalent points, a third one being hidden). The star of W contains five other points, chosen as indicated by the crosses; the corresponding six valleys are numbered as shown in the figure. The Γ point and representative X and L points are marked by full dots.

In the following, the invariant expansions of the effective-mass Hamiltonian at the W point for the most common fcc space groups: $Fm3m$ (e.g., lead), $Fd3m$ (e.g., germanium) and $F\bar{4}3m$ (e.g., zinc blende), are discussed including strain interactions for both the single-group (i.e., integer spin) and the double-group (i.e., half-integer spin) cases. In particular, the intervalley and intravalley splittings induced by a uniaxial stress along the principal symmetry directions [001], [011], and [111] are derived. Finally, several material parameters (masses and deformation potentials) appearing in those phenomenological expansions are evaluated for germanium by fitting the electronic bands near W as calculated with the *ab initio* linear-muffin-tin-orbital (LMTO) method in its fully relativistic form.[9,10]

II. INVARIANT EXPANSIONS AT THE W POINT

The expressions for the effective mass Hamiltonian at W presented here are derived by standard group-theoretical techniques taking time-reversal symmetry into account.[1,2] The (irreducible) star of W (see Fig. 1) contains six distinct points among which $W = (2\pi/a)(1,\frac{1}{2},0)$ is taken as representative.[11] In the invariant expansions, terms up to second order in the wave vector $\mathbf{k}$ (measured from the W point) and linear in the strain $\overleftrightarrow{\epsilon}$ are considered. For electrons, spin-orbit coupling is included as a perturbation. For the space groups $Fm3m$, $Fd3m$, and $F\bar{4}3m$, the acceptable irreducible representations (irreps) at the W point are either one or two dimensional (for the integer spin case, without counting the star degeneracy).[12,13] The effective-mass Hamiltonians for these nondegenerate or doubly degenerate bands are one or two dimensional. In the latter case, they are conveniently expressed in terms of the "orbital" matrices $\rho_0 = \left(\begin{smallmatrix}1&0\\0&1\end{smallmatrix}\right)$, $\rho_1 = \left(\begin{smallmatrix}1&0\\0&-1\end{smallmatrix}\right)$, $\rho_2 = \left(\begin{smallmatrix}0&1\\1&0\end{smallmatrix}\right)$, and $\rho_3 = \left(\begin{smallmatrix}0&-i\\i&0\end{smallmatrix}\right)$, acting on the partners of the single-group two-dimensional irreps. The usual notations $\sigma_x = \left(\begin{smallmatrix}0&1\\1&0\end{smallmatrix}\right)$, $\sigma_y = \left(\begin{smallmatrix}0&-i\\i&0\end{smallmatrix}\right)$, and $\sigma_z = \left(\begin{smallmatrix}1&0\\0&-1\end{smallmatrix}\right)$ are reserved for the spin matrices acting on the components of

the two-dimensional spinors, which are used when spin-orbit coupling is included. The size of the effective-mass Hamiltonian is then doubled; in which case, the notation $\rho_1\sigma_y$, for instance, represents the direct product of ρ_1 and σ_y, i.e., the four-dimensional matrix

$$\rho_1\sigma_y = \begin{pmatrix} 0 & -i & 0 & 0 \\ i & 0 & 0 & 0 \\ 0 & 0 & 0 & i \\ 0 & 0 & -i & 0 \end{pmatrix} .$$

Considering the symmorphic space group $Fm3m$ (O_h^5) to begin with, there are four one-dimensional and one two-dimensional single-group irreps at W.[13,14] For the two-dimensional irrep of the single group (W_3 in the notation of Ref. 14), the effective-mass Hamiltonian H (with the inclusion of strain and spin-orbit coupling) has the form[15]

$$H = \lambda\rho_0 + \beta\rho_1 + \gamma\rho_2 + \mu\rho_3 , \tag{1}$$

with

$$\lambda = \lambda_1 k_y^2 + \lambda_2(k_x^2 + k_z^2) + \lambda_3\epsilon_{yy} + \lambda_4(\epsilon_{xx} + \epsilon_{zz}) ,$$

$$\beta = \beta_1\sigma_y + \beta_2(\sigma_x k_x - \sigma_z k_z) ,$$

$$\gamma = \gamma_1 k_x k_z + \gamma_2\epsilon_{xz} ,$$

and

$$\mu = \mu_1 k_y + \mu_2(k_x^2 - k_z^2) + \mu_3(\epsilon_{xx} - \epsilon_{zz}) ;$$

here (and in similar expressions in the following), the real quantities $\lambda_1, \lambda_2, \ldots, \mu_3$ are material parameters (masses, deformation potentials, spin-orbit gaps), the y axis is singled out as a consequence of the choice $W = (2\pi/a)(1, \frac{1}{2}, 0)$ and, when spin-orbit coupling is neglected or phonons are considered, the terms involving the spin matrices (such as $\beta_1\sigma_y$) are to be omitted. The energy spectrum obtained diagonalizing H is given by

$$\begin{aligned} E_\pm = {} & \lambda_1 k_y^2 + \lambda_2(k_x^2 + k_z^2) + \lambda_3\epsilon_{yy} + \lambda_4(\epsilon_{xx} + \epsilon_{zz}) \\ & \pm[\beta_1^2 + \beta_2^2(k_x^2 + k_z^2) + \mu_1^2 k_y^2 + \mu_2^2(k_x^2 - k_z^2)^2 + \gamma_1^2 k_x^2 k_z^2 + 2\mu_1\mu_2 k_y(k_x^2 - k_z^2) + \gamma_2^2\epsilon_{xz}^2 + \mu_3^2(\epsilon_{xx} - \epsilon_{zz})^2 \\ & + 2\gamma_1\gamma_2\epsilon_{xz}k_x k_z + 2\mu_1\mu_3 k_y(\epsilon_{xx} - \epsilon_{zz}) + 2\mu_2\mu_3(k_x^2 - k_z^2)(\epsilon_{xx} - \epsilon_{zz})]^{1/2} ; \end{aligned} \tag{2}$$

in the presence of spin-orbit coupling H is a 4×4 matrix and each eigenvalue E_+ (E_-) is twofold degenerate as required by time reversal plus inversion symmetry;[1] for the spinless case, H is a 2×2 matrix and the eigenvalues are nondegenerate when $E_+ \neq E_-$ as given by Eq. (2) depending on $\mathbf{k}$ and $\overleftrightarrow{\epsilon}$. For instance, the strain-induced splittings at W in the case of phonons are obtained from Eq. (2), setting $\beta_1 = \beta_2 = 0$ and $\mathbf{k} = 0$,

$$E_\pm \rightarrow \lambda_3\epsilon_{yy} + \lambda_4(\epsilon_{xx} + \epsilon_{zz}) \pm \sqrt{\gamma_2^2\epsilon_{xz}^2 + \mu_3^2(\epsilon_{xx} - \epsilon_{zz})^2},$$

which gives an intravalley splitting for $\epsilon_{xz} \neq 0$ or $\epsilon_{xx} \neq \epsilon_{zz}$. For the integer spin case, Fig. 2 shows the intervalley and intravalley splittings induced by a uniaxial stress along high-symmetry directions.[16] When spin-orbit coupling is included, the intervalley splittings are the same and no intravalley splitting occurs as the strain cannot lift the double degeneracy required by time reversal plus inversion symmetry. The strain-induced intervalley splittings are as in Fig. 2 for every case considered here because they depend on how the symmetry of the fcc Bravais lattice is lowered and the star of W (possibly) becomes reducible. In particular, for uniaxial stress along a cubic axis [001] the deformed Bravais lattice is body-centered tetragonal, for stress along a dihedral axis [110] is body-centered orthorhombic, and for stress along a cubic diagonal [111] is rhombohedral. The intervalley splitting pattern at W corresponds to the following compact expression for the strain-induced energy shift ΔE_j of the valley at $\mathbf{K}_j$ ($j = 1, 2, \ldots, 6$, as in Fig. 1) with respect to the average shift of the six W valleys:

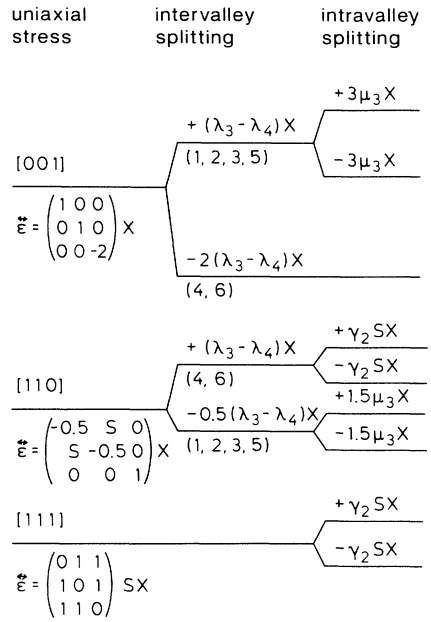

FIG. 2. Intervalley and intravalley splittings at W for the space group $Fm3m$ (integer spin case) induced by uniaxial stress along high-symmetry directions. The corresponding (traceless) strain tensors are shown, X being proportional to the externally applied stress and S a combination of elastic compliance constants [$S = \frac{1}{2}S_{44}/(S_{12} - S_{11})$]. The different valleys are identified by numbers according to Fig. 1 and other symbols are defined in the text [see Eq. (2)].

$$\Delta E_j = \left(\frac{a}{2\pi}\right)^2 (\lambda_4 - \lambda_3) \sum_{\mathbf{K}\simeq\mathbf{K}_j} \mathbf{K}\cdot(\overleftrightarrow{\epsilon} - \tfrac{1}{3}\mathrm{tr}\,\overleftrightarrow{\epsilon})\cdot\mathbf{K} ,$$

where the sum (for given j) is over the corresponding four equivalent wave vectors on the surface of the Brillouin zone, for instance (see Fig. 1), when $j = 1$ the sum is over $\mathbf{K} = (2\pi/a)(1,\frac{1}{2},0)$, $(2\pi/a)(-1,\frac{1}{2},0)$, $(2\pi/a)(0,-\frac{1}{2},1)$, and $(2\pi/a)(0,-\frac{1}{2},-1)$. The above expression for ΔE_j is analogous to those used for the intervalley splittings of the conduction minima in Si (along the Δ line) and Ge (at the L point), for which cases though the summation over equivalent points is not required.[17] For any one of the four one-dimensional (without counting spin) irreps at W (W_1, W_2, W_1', W_2' in the notation of Ref. 14), the effective mass Hamiltonian is simply

$$H = \lambda_1 k_y^2 + \lambda_2(k_x^2 + k_z^2) + \lambda_3\epsilon_{yy} + \lambda_4(\epsilon_{xx} + \epsilon_{zz}) ,$$

in particular, spin-orbit coupling does not split the double degeneracy, just as above; the strain-induced intervalley splittings are the same as above and, again, no intravalley splitting occurs.

Considering the nonsymmorphic space group $Fd3m$ (O_h^7) next, there are only two two-dimensional single-group irreps at W.[12,13,18] For either one of them (W_1, W_2 in the notation of Ref. 18), the Hamiltonian invariant expansion is

$$H = \lambda\rho_0 + \beta\rho_1 + \delta\rho_2 + \delta'\rho_3 , \tag{3}$$

with

$$\lambda = \lambda_1 k_y^2 + \lambda_2(k_x^2 + k_z^2) + \lambda_3\epsilon_{yy} + \lambda_4(\epsilon_{xx} + \epsilon_{zz}) ,$$
$$\beta = \beta_1\sigma_y + \beta_2(\sigma_x k_x - \sigma_z k_z) ,$$
$$\delta = \delta_1 k_x + \delta_2 k_y k_x + \delta_3\epsilon_{yx} ,$$

and

$$\delta' = -\delta_1 k_z + \delta_2 k_y k_z + \delta_3\epsilon_{yz} ;$$

the corresponding energy spectrum is

$$E_\pm = \lambda_1 k_y^2 + \lambda_2(k_x^2 + k_z^2) + \lambda_3\epsilon_{yy} + \lambda_4(\epsilon_{xx} + \epsilon_{zz}) \pm [\beta_1^2 + \beta_2^2(k_x^2 + k_z^2) + (\delta_1^2 + \delta_2^2 k_y^2)(k_x^2 + k_z^2) + 2\delta_1\delta_2 k_y(k_x^2 - k_z^2) + 2\delta_1\delta_3(k_x\epsilon_{yx} - k_z\epsilon_{yz}) + 2\delta_2\delta_3 k_y(k_x\epsilon_{yx} + k_z\epsilon_{yz}) + \delta_3^2(\epsilon_{yx}^2 + \epsilon_{yz}^2)]^{1/2} ; \tag{4}$$

as for $Fm3m$, when spin-orbit coupling is considered, each eigenvalue E_+ (E_-) is twofold degenerate; for the spinless case, the eigenvalues can be nondegenerate. In particular, for the case of phonons, the strain-induced splittings are obtained by setting $\beta_1 = \beta_2 = 0$ and $\mathbf{k} = 0$ in Eq. (4),

$$E_\pm \to \lambda_3\epsilon_{yy} + \lambda_4(\epsilon_{xx} + \epsilon_{zz}) \pm |\delta_3|\sqrt{\epsilon_{yx}^2 + \epsilon_{yz}^2} ;$$

therefore, while the intervalley splittings are the same as in Fig. 2, the intravalley splitting pattern is different, as shown in Fig. 3. When spin-orbit coupling is included, the strain-induced splittings are analogous to those of $Fm3m$ discussed above.

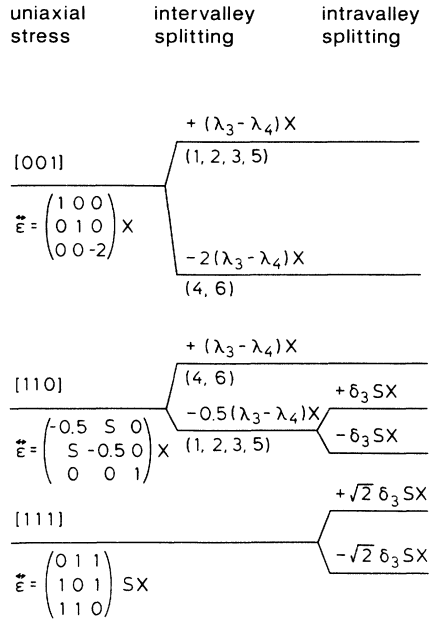

FIG. 3. Same as Fig. 2 for the space group $Fd3m$ [see Eq. (4)].

Considering the symmorphic space group $F\bar{4}3m$ (T_d^2) at last, there are four one-dimensional single-group irreps at W.[13,19,20] For any one of them (W_1, W_2, W_3, W_4 in the notation of Ref. 20), the Hamiltonian invariant expansion is

$$H = \lambda_1 k_y^2 + \lambda_2(k_x^2 + k_z^2) + \lambda_3\epsilon_{yy} + \lambda_4(\epsilon_{xx} + \epsilon_{zz}) + \beta_1\sigma_y + \beta_2(k_x\sigma_x - k_z\sigma_z) , \tag{5}$$

with eigenvalues

$$E_\pm = \lambda_1 k_y^2 + \lambda_2(k_x^2 + k_z^2) + \lambda_3\epsilon_{yy} + \lambda_4(\epsilon_{xx} + \epsilon_{zz}) \pm\sqrt{\beta_1^2 + \beta_2^2(k_x^2 + k_z^2)} ; \tag{6}$$

in particular, the spin-orbit interaction removes the twofold degeneracy as a consequence of the lack of inversion symmetry in this group.[6,9] The strain-induced intervalley splittings are the same as in Figs. 2 and 3.

III. NUMERICAL RESULTS FOR GERMANIUM

In the following, the case of germanium (space group $Fd3m$) is studied to illustrate the use and range of validity of the invariant expansions presented above. The material parameters appearing in the effective-mass Hamiltonian at W [Eqs. (3) and (4), including spin-orbit terms] are varied in order to reproduce the electronic bands near W as calculated (with and without strain) by means of the fully relativistic LMTO method.[9,10,21]

The LMTO method is based on the local-density approximation and thus suffers from the well-known "band-gap problem," i.e., the conduction state energies are notoriously underestimated. This deficiency is cured by in-

cluding *ad hoc* potentials in the self-consistent iteration scheme and by adjusting them to obtain good agreement with experimental excitation energies.[9] Spin-orbit interaction is treated as a perturbative term in the LMTO Hamiltonian.

In the unstrained crystal, the uppermost valence levels at W occur at[22] $V_1 = -4.752$ eV and $V_2 = -4.670$ eV, V_1 and V_2 are each doubly degenerate and correspond to the same single-group two-dimensional irrep; the difference $V_2 - V_1$ is the valence-band spin-orbit splitting at W, from which the value $|\beta_1^{(V)}| \simeq 41$ meV is obtained. The case of the conduction band is analogous with levels at $C_1 = +3.700$ eV and $C_2 = +3.847$ eV, which gives $|\beta_1^{(C)}| \simeq 73$ meV. The dispersion relations in the vicinity of W along the directions WX from W to X and WL from W to L (see Fig. 1) are shown in Figs. 4(a) and 4(b) for the valence and conduction bands, respectively. The solid lines represent Eq. (4) with parameters varied to reproduce the LMTO results (dots) in a range of about 1% of the Brillouin zone around W (indicated by arrows in Fig. 4). Setting $\lambda_1 = \hbar^2/2m_{\|}$, $\lambda_2 = \hbar^2/2m_{\perp}$ and $(2\pi/a)\sqrt{\delta_1^2 + \beta_2^2} = \Lambda$, this fit gives for the valence band $m_{\|}^{(V)} \simeq +0.82m_0$, $m_{\perp}^{(V)} \simeq +0.71m_0$, $\Lambda^{(V)} \simeq 3.0$ eV, and for the conduction band $m_{\|}^{(C)} \simeq -0.037m_0$, $m_{\perp}^{(C)} \simeq -0.22m_0$, $\Lambda^{(C)} \simeq 4.3$ eV. The masses as calculated with the LMTO method typically agree within 20% with experimental results, usually overestimating them.[23] With the same parameters, Eq. (4) reproduces the LMTO bands over a range of at least 5% of the Brillouin zone around W, as shown in Fig. 4. The masses are electronlike (i.e., positive) for the valence band and holelike (i.e., negative) for the conduction band (for the latter case, they are strongly anisotropic). Along the WL direction, the dispersion is dominated by the term proportional to Λ. This term, in the case of phonons or when spin-orbit coupling is neglected, is responsible for a slope discontinuity at W, accompanied by a dispersion linear in $\mathbf{k}$ along the plane perpendicular to the WX direction.[24] The quoted parameter values are to be used in conjunction with Eq. (4), with vanishing $\overleftrightarrow{\epsilon}$; in particular, along the WL direction a simple parabolic expression neglecting the Λ term would not be appropriate.

The effects induced by a uniaxial stress along the z cubic axis [001] are considered next.[25] The corresponding intervalley splittings [i.e., the difference between energies at $(2\pi/a)(1, \frac{1}{2}, 0)$ and at $(2\pi/a)(0, 1, \frac{1}{2})$; see Fig. 3] are shown in Figs. 5(a) and 5(b) for the valence (V_1, open dots; V_2, closed dots) and conduction (C_1, open dots; C_2, closed dots) bands, respectively. The solid lines represent Eq. (4) with $\mathbf{k}=0$ and $(\lambda_3 - \lambda_4)$ varied to reproduce the average valence- or conduction-band splittings for strain values up to about 0.2% (range indicated by arrows in Fig. 5); this fit gives for the valence band $(\lambda_3^{(V)} - \lambda_4^{(V)}) \simeq -0.51$ eV and for the conduction band $(\lambda_3^{(C)} - \lambda_4^{(C)}) \simeq -15$ eV. The intervalley splittings are well described by this linear expression at least for strains up to 1% in the conduction-band case, whereas deviations from linearity due to higher-order terms not included in Eq. (3) appear in the valence-band case.[26]

When a uniaxial strain is applied along the main cubic diagonal [111], the spin-orbit splittings at W increase according to Eq. (4):

$$E_+ - E_- = 2[\beta_1^2 + \delta_3^2(\epsilon_{yx}^2 + \epsilon_{yz}^2)]^{1/2} . \quad (7)$$

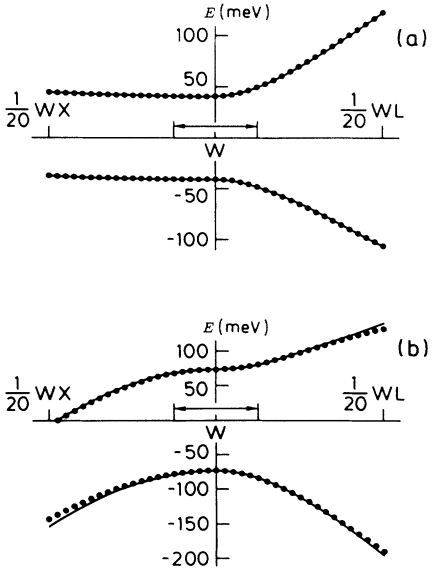

FIG. 4. Germanium (a) valence- and (b) conduction-band dispersion relations [$E(\mathbf{k})$] near the W point along the WL (at the right) and WX (at the left) directions, see text for details.

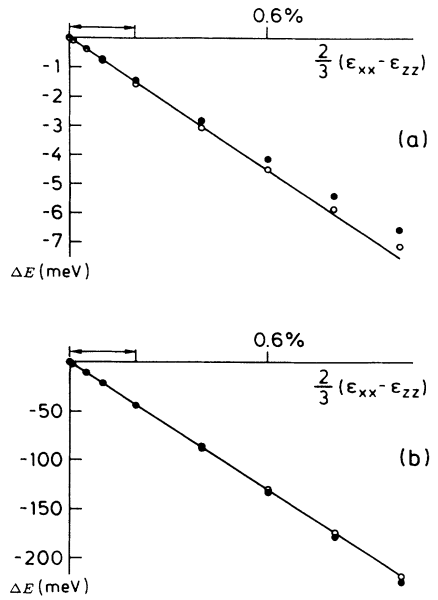

FIG. 5. Germanium (a) valence and (b) conduction W-point intervalley splittings (ΔE) for uniaxial stress along the z cubic axis [001], see text for details.

In this case, the atomic positions in the trigonally distorted crystal are not simply given by the affine transformation describing the distortion of the unit cell because the second atom in the basis [at $(a/4)(1,1,1)$] can also be displaced as in a longitudinal-optic phonon along [111]. This additional degree of freedom is described by the internal strain parameter ζ that varies between 0, corresponding to the affine deformation only, and 1, corresponding to keeping the distance between the two nearest neighbors along [111] equal to that in the unstrained crystal.[27] The LMTO bands can be calculated for any given value of the internal strain parameter.[28] As above, the parameter $|\delta_3|$ is obtained by fitting Eq. (7) to the calculated bands, which gives for the valence band $|\delta_3^{(V)}| \simeq 2.0$ eV with ζ=0 and $|\delta_3^{(V)}| \simeq 1.5$ eV with ζ=1, and for the conduction band $|\delta_3^{(C)}| \simeq$16 eV with ζ=0 and $|\delta_3^{(C)}| \simeq 19$ eV with ζ=1; intermediate values of ζ have also been considered. The corresponding values of $|\delta_3|$ are well described by a linear interpolation between ζ=0 and 1 for the conduction band. For the valence band, instead, the values of $|\delta_3|$ for intermediate values of ζ are considerably smaller than those for either ζ=0 or 1; in particular, for $\zeta \simeq 0.58$ (which is most appropriate for Ge, see Ref. 27), the strain-induced variation of the valence-band spin-orbit splitting is very small and no longer described by Eq. (7) [i.e., $|\delta_3^{(V)}(\zeta \simeq 0.58)| \simeq 0$]. In fact,[29] δ_3 contains both the contribution of the affine deformation [δ_3(af)] and of the optical phonon [δ_3(ph)]: $\delta_3 = \delta_3(\mathrm{af}) - \frac{1}{4}\zeta\delta_3(\mathrm{ph})$; in the case of the valence band, δ_3 as a function of ζ changes sign for $\zeta \simeq 0.58$.

Finally, it is worth mentioning that the invariant expansions presented here are by no means limited to the phonon or electron case, but can be used to describe the dispersion around the W point of any (integer or half-integer) excitation, including strain-induced effects, as long as the underlying crystal space-group symmetry and time-reversal invariance are not broken.[30]

ACKNOWLEDGMENTS

It is a pleasure to thank S. Zollner for many useful discussions. One of the authors (G.C.L.R.) gratefully acknowledges support from the Alexander von Humboldt-Stiftung (Bonn, Germany). The LMTO calculations have been performed at "Höchstleistungsrechenzentrum für Wissenschaft und Forschung" (Jülich, Germany), with a computer program written by N. E. Christensen, whom we also thank for valuable discussions.

[1] F. Bassani and G. Pastori Parravicini, *Electronic States and Optical Transitions in Solids* (Pergamon, Oxford, 1975).
[2] G. L. Bir and G. E. Pikus, *Symmetry and Strain-Induced Effects in Semiconductors* (Wiley, New York, 1974).
[3] J. M. Luttinger, Phys. Rev. **102**, 1030 (1956).
[4] F. H. Pollak and M. Cardona, Phys. Rev. **172**, 816 (1968).
[5] A. K. Ramdas and S. Rodriguez, in *Progress on Electron Properties of Solids*, edited by R. Girlanda *et al.* (Kluwer Academic, Dordrecht, 1989).
[6] N. Kim, G. C. La Rocca, S. Rodriguez, and F. Bassani, Riv. Nuovo Cimento **12**, 2 (1989).
[7] J. C. Phillips, Phys. Rev. **113**, 147 (1959).
[8] See, for instance, the discussion concerning electron pockets at W in the fourth zone of lead by W. Joss, Phys. Rev. B **23**, 4913 (1981), or the discussion concerning a 2TA(W) overtone in the second-order Raman spectrum of GaP by B. A. Weinstein and G. J. Piermarini, Phys. Lett. **48A**, 14 (1974).
[9] U. Schmid, N. E. Christensen, and M. Cardona, Phys. Rev. B **41**, 5919 (1990).
[10] U. Schmid, N. E. Christensen, and M. Cardona, Solid State Commun. **75**, 39 (1990).
[11] Unless explicitly stated, W always refers to this specific choice.
[12] In the case of nonsymmorphic groups (such as $Fd3m$) and points on the boundary of the Brillouin zone (such as W), the acceptable irreps correspond to projective representations.
[13] *Kronecker Product Tables*, edited by A. P. Cracknell, B. L. Davies, S. C. Miller, and W. F. Love (IFI/Plenum, New York, 1979), Vol. 1.
[14] L. P. Bouckaert, R. Smoluchowski, and E. Wigner, Phys. Rev. **50**, 58 (1936).
[15] Here and in similar equations in the following, the explicit matrix form of H (obtained using the expressions for the ρ's and σ's given in the text) implies a specific choice of basis functions; which, however, is immaterial for our purposes as the energy eigenvalues are independent of this choice. In the case of Eq. (1), for instance, the basis functions of the W_3 irrep can be taken as $i(x+iz)$ and $(x-iz)$; see also Ref. 2, Secs. 25 and 26.
[16] Equation (2) is written for the reference valley at $(2\pi/a)(1,\frac{1}{2},0)$, but strain-induced effects at any other valley (and thus intervalley splittings) are easily derived making use of cubic symmetry. For instance, the effects of uniaxial stress along z on the valley at $(2\pi/a)(0,1,\frac{1}{2})$ are the same as those of uniaxial stress along y on the reference valley.
[17] H. Brooks, in *Advances in Electronic and Electron Physics*, edited by L. Marton (Academic, New York, 1955), Vol. 7.
[18] R. J. Elliott, Phys. Rev. **96**, 280 (1954).
[19] R. H. Parmenter, Phys. Rev. **100**, 573 (1955).
[20] G. Dresselhaus, Phys. Rev. **100**, 580 (1955).
[21] The invariant expansions of Sec. II have been also used with similar results to fit the electronic bands of several other diamondlike or zinc-blende-like semiconductors (with uniaxial stress in different directions) as calculated by an empirical pseudo-potential method with relativistic corrections. The relative code has been made available to us by courtesy of S. Zollner.
[22] The zero of the energy scale is at the top of the valence band at Γ.
[23] M. Cardona, N. E. Christensen, and G. Fasol, Phys. Rev. B **38**, 1806 (1988).
[24] See also, F. A. Johnson and R. Loudon, Proc. R. Soc. London, Ser. A **281**, 274 (1964), especially Fig. 1 therein.
[25] For the case of uniaxial stress along a cubic axis, the LMTO deformation potentials for which measurements have been

performed are in excellent agreement with experiment, see Ref. 10.

[26] In particular, the difference between the intervalley splittings of the V_2 and V_1 bands is due to spin-dependent strain interactions, i.e., invariant terms involving combinations of $\overleftrightarrow{\epsilon}$ and σ.

[27] P. Molinàs-Mata and M. Cardona, Phys. Rev. B **43**, 9799 (1991).

[28] N.E. Christensen, Solid State Commun. **50**, 177 (1984).

[29] M. Cardona, in *Light Scattering in Solids II*, edited by M. Cardona and G. Guentherodt (Springer, Berlin, 1982).

[30] Quite recently [see K. M. Leung and Y. F. Liu, Phys. Rev. Lett. **65**, 2646 (1990); also, Z. Zhang and S. Satpathy, *ibid.* **65**, 2650 (1990), and K.M. Ho, C.T. Chan, and C.M. Soukoulis, *ibid.* **65**, 3152 (1990)], it has been predicted that a true gap is absent in the photonic band structure of a face-centered-cubic dielectric crystal (space group $Fm3m$) due to a sticking together of valence and conduction bands at the W point. This degeneracy is required by symmetry when no inversion of energy levels occurs with respect to the free-photon vector-plane-wave band structure, as easily seen from the compatibility relations with the conduction- and valence-band irreps at the X point (X_5 and X_5', in the notations of Ref. 14). In this case, as shown in Fig. 2, a gap at W is opened by a rhombohedral distortion, such as a [111] uniaxial stress.